the sixth coordination site, which to our knowledge is the first example of an agostic C–H interaction in a classical coordination complex. NMR studies of **3** are consistent with a weak agostic interaction, since only a slightly reduced ^{13}C–H coupling constant is observed for the agostic C–H group. The weakness of the Co···HC interaction and the reason for the surprising stability of **3** in aqueous solution is attributed to the strong trans influence of the sulfite ligand. Nevertheless, the agostic interaction in **3** activates the C(2)–H(2a) bond sufficiently such that it can be deprotonated in methanol to give Co–alkyl complex **5**. This demonstrated activation of a C–H bond via electrophilic attack of Co(III) strongly supports the mechanism shown in Scheme I, which was proposed earlier[4] for the general preparation of **5**. It is intriguing that a relatively simple but sterically constrained molecule can exhibit C–H activation in an aqueous environment. Such specificity may be inherent to C–H activation in enzymes.

Acknowledgment. We are grateful to Don Appel for assistance in obtaining the NMR spectra. We also wish to thank Professor Hisahiko Einaga of University of Tsukuba and Professor Nobuko Matsuoka of Osaka University for technical assistance. The Nicolet X-ray diffractometer was acquired with the aid of NSF Grant CHE-8408407 and The Boeing Corp. In addition, The Boeing Corp. is gratefully acknowledged for assistance in obtaining the Nicolet 200-MHz NMR spectrometer.

Supplementary Material Available: For **3**, tables of complete positional and thermal parameters including those of H atoms, anisotropic thermal parameters, bond distances and bond angles, and data collection and refinement parameters (10 pages); a listing of F_o and F_c values (24 pages). Ordering information is given on any current masthead page.

Contribution from the School of Chemical Sciences and Materials Research Laboratory, University of Illinois, Urbana, Illinois 61801

Synthesis, Structural Characterization, and Photoinduced Hydrogenation of $[PPN]_2[Re_6C(CO)_{19}]$

Gishun Hsu, Scott R. Wilson, and John R. Shapley*

Received May 30, 1990

Treatment of $[PPN]_3[Re_7C(CO)_{21}]$ with 2 equiv of ferrocenium ion in the presence of excess triphenylphosphine and a carbon monoxide atmosphere provided $[PPN]_2[Re_6C(CO)_{19}]$, which was isolated as a crystalline solid in 90% yield. The coproduct was identified as $[Re(CO)_4(PPh_3)_2]^+$. $[Et_4N]_2[Re_6C(CO)_{19}]$ was prepared in similar yield. The compound $[PPN]_2[Re_6C(CO)_{19}]$ crystallizes in the monoclinic space group $I2/a$ with a = 23.943 (10) Å, b = 14.907 (6) Å, c = 26.164 (9) Å, β = 93.75 (3)°, and Z = 4 (at T = −125 °C). The octahedral Re_6C core has crystallographically imposed C_2 symmetry. There are 18 terminal carbonyl ligands, three coordinated to each metal atom. Two unique positions exist for the 19th carbonyl ligand: one is symmetrically edge bridging, and the second is nearly terminal but with weak bridging interactions to the adjacent two rhenium atoms defining a triangular face. Solution ^{13}C NMR spectra of $[PPN]_2[Re_6{}^{13}C(^{13}CO)_{19}]$ (ca. 50% ^{13}C) showed complete scrambling of the carbonyl ligands even at −85 °C. The averaged ^{13}C–^{13}C coupling between the carbide ligand and the carbonyl ligands was observed as ^2J = 2.6 Hz. Sunlamp irradiation of $[PPN]_2[Re_6C(CO)_{19}]$ in the presence of hydrogen gas gave $[PPN]_2[H_2Re_6C(CO)_{18}]$ in high yield.

Introduction

In 1985 Beringhelli et al.[1] reported that oxidation of the capped-octahedral[2] rhenium cluster $[Re_7C(CO)_{21}]^{3-}$ with a stoichiometric amount of iodine (acetonitrile, room temperature, CO atmosphere) resulted in removal of the capping $Re(CO)_3$ unit to give $[Re_6C(CO)_{19}]^{2-}$ and that excess iodine provided the novel species $[Re_4C(CO)_{15}I]^-$ in low yield. A footnote to this paper mentioned a preliminary X-ray crystallographic analysis of $[Re_6C(CO)_{19}]^{2-}$ that showed the complex was "an octahedral cluster, centered by the carbide, bearing one doubly-bridging and eighteen terminal CO groups, three for each Re atom." However, no further preparative or structural details regarding $[Re_6C(CO)_{19}]^{2-}$ have been published. As part of our interest in the formation and interconversion of large rhenium carbonyl clusters,[3,4] we have developed a new synthesis of $[Re_6C(CO)_{19}]^{2-}$. In this paper, we report that the reaction of $[Re_7C(CO)_{21}]^{3-}$ with ferrocenium ion (Cp_2Fe^+) in the presence of excess triphenylphosphine and carbon monoxide provides $[Re_6C(CO)_{19}]^{2-}$ in 90% isolated yield together with an identified mononuclear coproduct (eq 1). The structure of $[PPN]_2[Re_6C(CO)_{19}]$ has been fully defined by a low-temperature single-crystal X-ray crystallographic study. Furthermore, we describe the unique photoreactivity of $[Re_6C(CO)_{19}]^{2-}$, which in the presence of hydrogen gas gives the previously known[3,5] dihydrido complex $[H_2Re_6C(CO)_{18}]^{2-}$ (eq 2).

$$[Re_7C(CO)_{21}]^{3-} \xrightarrow[PPh_3,\ CO]{2\ Cp_2Fe^+} [Re_6C(CO)_{19}]^{2-} + [Re(CO)_4(PPh_3)_2]^+ \quad (1)$$

$$[Re_6C(CO)_{19}]^{2-} + H_2 \xrightarrow{h\nu} [H_2Re_6C(CO)_{18}]^{2-} + CO \quad (2)$$

Experimental Section

General Procedures. All operations were conducted by using standard Schlenk techniques. The $[(Ph_3P)_2N]^+$ (PPN^+) and $[Et_4N]^+$ salts of $[Re_7C(CO)_{21}]^{3-}$ were prepared as described previously.[3] Triphenylphosphine and $[Cp_2Fe][PF_6]$ were obtained commercially and were used without further purification. Acetone, dichloromethane, and THF were distilled under nitrogen from anhydrous potassium carbonate, calcium hydride, and sodium/benzophenone, respectively. Triglyme was dried by stirring over sodium at 120 °C under nitrogen for 2 days and was distilled before use. Infrared (IR) spectra were recorded on a Perkin-Elmer 1750 FT-IR spectrometer. Elemental analyses were determined in the Microanalytical Laboratory of the School of Chemical Sciences. Fast atom bombardment (FAB) mass spectra were obtained in the School Mass Spectrometry Laboratory; the matrix used was "Magic Bullet" (dithioerythritol–dithiothreitol). ^{13}C NMR spectra were recorded in acetone-d_6 and are referenced to the carbonyl resonance at δ 206.0. High-resolution spectra were obtained on a General Electric GN-500 spectrometer at 125 MHz by using a 128 K data set, which corresponds to a digital resolution of 0.54 Hz/point. Variable-temperature spectra were measured on a General Electric QE-300 spectrometer at 75 MHz.

Preparation of $[PPN]_2[Re_6C(CO)_{19}]$. To a flask containing $[PPN]_3[Re_7C(CO)_{21}]$ (169 mg, 0.0480 mmol), $[Cp_2Fe]PF_6$ (35 mg, 0.11 mmol), and triphenylphosphine (512 mg, 1.95 mmol) was added acetone (50

(1) Beringhelli, T.; Ciani, G.; D'Alfonso, G.; Sironi, A.; Freni, M. *J. Chem. Soc., Chem. Commun.* **1985**, 978.
(2) Ciani, G.; D'Alfonso, G.; Freni, M.; Romiti, P.; Sironi, A. *J. Chem. Soc., Chem. Commun.* **1982**, 339.
(3) Hayward, C.-M. T.; Shapley, J. R. *Organometallics* **1988**, *7*, 448.
(4) Henley, T. J.; Wilson, S. R.; Shapley, J. R. *Organometallics* **1987**, *6*, 2618.
(5) Ciani, G.; D'Alfonso, G.; Romiti, P.; Sironi, A.; Freni, M. *J. Organomet. Chem.* **1983**, *244*, C27.
(6) Angelici, R. J.; Brink, R. W. *Inorg. Chem.* **1973**, *12*, 1067.

0020-1669/91/1330-3881$02.50/0

mL). After all solids dissolved (5 min), a carbon monoxide atmosphere was introduced, and the solution was stirred at ambient temperature for 6 h. The color of the solution changed from crimson to burgundy red. The IR (ν_{CO}) spectrum of the solution showed only bands due to $[Re_6C(CO)_{19}]^{2-}$ and to $[Re(CO)_4(PPh_3)_2]^+$ (vide infra). The solvent was removed in vacuo, and the solid residue was washed first with 2-propanol and then with diethyl ether. Crystallization of the residue by solvent diffusion with dichloromethane/2-propanol provide red crystals of $[PPN]_2[Re_6C(CO)_{19}]$ (118 mg, 0.0430 mmol, 90%), which were separated and dried in vacuo. Anal. Calcd for $C_{92}H_{60}N_2O_{19}P_4Re_6$: C, 40.35; H, 2.21; N, 1.02. Found: C, 40.34; H, 2.20; N, 1.03. IR (dichloromethane): ν_{CO} 2051 (vw), 1991 (vs), 1976 (s), 1905 (w), 1895 (w, sh), 1815 (vw) cm^{-1}. IR (KBr): ν_{CO} 2050 (vw), 1988 (s, sh), 1983 (vs), 1968 (vs), 1894 (m), 1810 (w) cm^{-1}. ^{13}C NMR (125 MHz, acetone-d_6, 20 °C): δ 417.9 (s, 1 C, μ_6-C), 198.0 (s, 19 C). Negative ion FAB mass spectrum (^{187}Re): m/z 2204 ($[PPN][Re_6C(CO)_{19}]$), 2176 ($[PPN][Re_6C(CO)_{19}$-CO]), 1666 ($Re_6C(CO)_{19}$), 1638 ($Re_6C(CO)_{19}$ - CO).

$[PPN]_2[Re_6{}^{13}C(^{13}CO)_{19}]$ was prepared from $[PPN]_3[Re_7{}^{13}C(^{13}CO)_{21}]$ (ca. 50% ^{13}C) by employing an atmosphere of nitrogen instead of carbon monoxide; the yield was 71%.

Identification of *trans*-$[Re(CO)_4(PPh_3)_2]^+$. The filtrates from the crystallization of several samples of $[PPN]_2[Re_6C(CO)_{19}]$ were combined. After concentration of the solution and several recrystallizations of the resulting precipitate, $[Re(CO)_4(PPh_3)_2]^+$ salts could be separated from residual $[Re_6C(CO)_{19}]^{2-}$. IR (dichloromethane): ν_{CO} 2110 (w), 2031 (w), 2006 (vs) cm^{-1} (lit.[6] ν_{CO} 2109 (vw), 2033 (w), 2004 (vs) cm^{-1}). Positive-ion FAB mass spectrum (^{187}Re): m/z 823 ($Re(CO)_4(PPh_3)_2$), 823 - 28x, x = 1, 2 ($Re(CO)_4(PPh_3)_2$ - xCO).

Preparation of $[Et_4N]_2[Re_6C(CO)_{19}]$. $[Et_4N]_3[Re_7C(CO)_{21}]$ (111 mg, 0.0484 mmol), $[Cp_2Fe]PF_6$ (35 mg, 0.11 mmol), and triphenylphosphine (499 mg, 1.90 mmol) were dissolved in acetone (50 mL). A carbon monoxide atmosphere was introduced, and the reaction mixture was stirred at ambient temperature for 5 h. The solution was evaporated to dryness, and the residue was washed with 2-propanol and diethyl ether. Crystallization from acetone/2-propanol gave red needles of $[Et_4N]_2[Re_6C(CO)_{19}]$ (84 mg, 0.044 mmol, 90%). Anal. Calcd for $C_{36}H_{40}N_2O_{19}Re_6$: C, 22.50; H, 2.10; N, 1.46. Found: C, 22.69; H, 2.12; N, 1.47. Negative ion FAB mass spectrum (^{187}Re): m/z 1666 ($Re_6C(CO)_{19}$), 1638 (($Re_6C(CO)_{19}$) - CO).

Preparation of $[PPN][Re_7C(CO)_{22}]$. To a flask containing $[PPN]_3[Re_7C(CO)_{21}]$ (571 mg, 0.162 mmol) and $[Cp_2Fe]PF_6$ (119 mg, 0.359 mmol) was transferred dichloromethane (200 mL) via cannula. Carbon monoxide was bubbled through the solution for 10 min, during which time the solution color changed to bright red. After evaporation of the solvent, the residual solid was first washed with hexane and then extracted with ether (5 × 100 mL), leaving a residue of $[PPN][PF_6]$. Evaporation of the ether solution provided a red powder, which gave red needles of $[PPN][Re_7C(CO)_{22}]$ (357 mg, 0.145 mmol, 89%) after crystallization from dichloromethane/cyclohexane. Anal. Calcd for $C_{59}H_{30}NO_{22}P_2Re_7$: C, 28.69; H, 1.22; N, 0.57. Found: C, 28.91; H, 1.52; N, 0.57. IR (dichloromethane): ν_{CO} 2080 (vw), 2030 (vs), 2017 (s), 2005 (m, sh), 1996 (mw, sh), 1953 (w), 1913 (w), 1843 (vw) cm^{-1} (lit.[7] ν_{CO} 2080 (vw), 2032 (vs), 2018 (s), 2005 (sh), 1995 (sh), 1950 (mw) 1910 (mw), 1850 (vw) cm^{-1}). Negative ion FAB mass spectrum (^{187}Re): m/z 1937 ($Re_7C(CO)_{22}$), 1937 - 28x, x = 1-8 ($Re_7C(CO)_{22}$ - xCO).

Decapping of $[Re_7C(CO)_{22}]^-$ with Triphenylphosphine. $[PPN]_3[Re_7C(CO)_{21}]$ (154 mg, 0.0436 mmol) and $[Cp_2Fe]PF_6$ (33 mg, 0.010 mmol) were dissolved in dichloromethane (100 mL), and then carbon monoxide was bubbled through the solution for 5 min. The only IR bands observed were those of $[Re_7C(CO)_{22}]^-$. The solvent was evaporated, and the solid residue was washed with hexane to remove ferrocene. Triphenylphosphine (590 mg, 2.24 mmol) and acetone (100 mL) were added, and the reaction solution was stirred for 48 h at ambient temperature. Only the IR bands for $[Re_7C(CO)_{22}]^-$ and $[Re_6C(CO)_{19}]^{2-}$ were observed during the course of the reaction. After evaporation of the solvent, the residual solid was washed with ether, and crystallization from acetone/2-propanol gave $[PPN]_2[Re_6C(CO)_{19}]$ (107 mg, 0.0390 mmol, 90%). The use of greater than 20 equiv of PPh_3 was necessary for complete conversion of $[Re_7C(CO)_{22}]^-$. The formation of $[Re_6C(CO)_{19}]^{2-}$ could not be effected in dichloromethane.

Note Added in Proof. $[PPN][Re_7C(CO)_{22}]$ also undergoes decapping in acetonitrile in the absence of triphenylphosphine. Addition of [PPN]Cl and crystallization from acetonitrile/2-propanol gave $[PPN]_2[Re_6C(CO)_{19}]$ in 73% yield.

Attempted Thermally Induced Hydrogenation of $[PPN]_2[Re_6C(CO)_{19}]$. $[PPN]_2[Re_6C(CO)_{19}]$ (10 mg) was dissolved in triglyme (25 mL), and hydrogen was bubbled through the solution as it was heated in stages at 50, 100, 150, and 200 °C. At 50 and 100 °C, no change in the IR spectrum of the solution was seen after 2 h of heating. At 150 °C, several additional IR bands were observed after 30 min of heating, but none could be attributed to a known rhenium cluster compound. At 200 °C, cluster decomposition was more rapid, and a profusion of unassigned IR bands appeared.

Table I. Crystallographic Data for $[PPN]_2[Re_6C(CO)_{19}]\cdot 2C_3H_6O$

formula	$C_{92}H_{60}N_2O_{19}P_4Re_6\cdot 2C_3H_6O$	fw	2738.59 + 116.16
		temp, °C	-125
space group	$I2/a$ (No. 15), monoclinic	λ, Å	0.71073 (Mo Kα)
		ρ_{calcd}, g cm^{-3}	2.035
a, Å	23.943 (10)	μ, cm^{-1}	80.09
b, Å	14.907 (6)	transm coeff	0.141-0.048
c, Å	26.164 (9)	R^a	0.068
β, deg	93.75 (3)	$R_w{}^b$	0.078
V, Å^3	9318 (11)		
Z	4		

$^a R = \sum||F_o| - |F_c||/\sum|F_o|$. $^b R_w = [\sum w(|F_o| - |F_c|)^2/\sum w|F_o|^2]^{1/2}$, where $w = k/([\sigma(F_o)]^2 + [pF_o]^2)$ and k = 2.78 and p = 0.020.

Photoinduced Hydrogenation of $[PPN]_2[Re_6C(CO)_{19}]$. At room temperature, hydrogen was bubbled through a dichloromethane solution (25 mL) of $[PPN]_2[Re_6C(CO)_{19}]$ (11 mg, 0.0038 mmol) contained in a Pyrex flask. After 30 min of irradiation with a sunlamp (GE 275 W), the only IR bands observed were those attributable to $[H_2Re_6C(CO)_{18}]^{2-}$. After evaporation of the solvent, crystallization of the residue from THF/2-propanol gave $[PPN]_2[H_2Re_6C(CO)_{18}]$ (9 mg, 0.0033 mmol, 87%). Anal. Calcd for $C_{91}H_{62}N_2O_{18}P_4Re_6$: C, 40.29; H, 2.30; N, 1.03. Found: C, 40.01; H, 2.62; N, 0.92. IR (acetone): ν_{CO} 1997 (s, sh), 1985 (vs), 1928 (w, sh), 1905 (m) cm^{-1} (lit.[5] ν_{CO} 1997 (s, sh), 1983 (vs), 1925 (w), 1900 (m) cm^{-1}).

X-Ray Crystallographic Study. Crystals of $[PPN]_2[Re_6C(CO)_{19}]$ suitable for diffraction studies were grown by diffusion of 2-propanol into an acetone solution over a period of 7 days at ambient temperature. A dark red crystal (dimensions 0.4 × 0.4 × 0.5 mm) was mounted with an oil (Paratone-N, Exxon) to a thin glass fiber. Data collection was carried out at -125 °C on an Enraf-Nonius CAD4 automated κ-axis diffractometer. Pertinent crystallographic data are summarized in Table I. Unit cell parameters were obtained by a least-squares fit of 25 machine-centered reflections (25° < 2θ < 36°). A total of 7727 independent reflections, 4976 observed with $I > 2.58\sigma(I)$, in the range 2° < 2θ < 49° were measured at variable rates over a period of 82 h with no change in the appearance of the sample. Data were corrected numerically for absorption and for anomalous dispersion, Lorentz, and polarization effects.

The structure was solved by direct methods (SHELXS-86); correct positions for the rhenium atoms were deduced from an E map. Subsequent least-squares difference Fourier calculations (SHELX-76) revealed positions for the remaining non-hydrogen atoms. Twofold symmetry was imposed on the disordered anion; no crystallographic symmetry was imposed on the cation. Phenyl rings and the disordered solvate molecule were constrained to idealized geometry. Hydrogen atoms on the disordered solvate molecule were not included in the structure factor calculations. In the final cycle of least-squares refinement, anisotropic thermal coefficients were refined for the rhenium, phosphorus, and nitrogen atoms. Common isotropic thermal parameters were varied for the hydrogen, solvate, and carbonyl carbon and oxygen atoms, and the remaining non-hydrogen atoms were refined with isotropic thermal coefficients. Owing to high correlation coefficients, terminal Re-C(-O) bond lengths were constrained. The choice of space group was confirmed by the average values of the normalized structure factors and by successful refinement of the proposed model in the centric space group. The highest peaks in the final difference Fourier map were in the vicinity of the rhenium positions, +1.98 e/Å^3. Final agreement factors were R = 0.068, R_w = 0.078, and "goodness of fit" = 2.11 for 494 parameters and an observable/parameter ratio of 10.1. Positional parameters for the cluster anion are listed in Table II, and selected bond distances and angles are displayed in Table III. Complete lists of atom coordinates, thermal coefficients, and bond distances and bond angles are provided as supplementary material.

Results

The oxidation of $[Re_7C(CO)_{21}]^{3-}$ in acetone with 2 equiv of $[Cp_2Fe]^+$ in the presence of carbon monoxide and 20-40 equiv of triphenylphosphine provides $[Re_6C(CO)_{19}]^{2-}$ together with $[Re(CO)_4(PPh_3)_2]^+$. The isolated yields of either $[PPN]_2[Re_6C(CO)_{19}]$ or $[NEt_4]_2[Re_6C(CO)_{19}]$ are 90%, but the yield drops somewhat (to 71%) when the reaction is conducted under a nitrogen atmosphere instead. Analogous oxidation of $[PPN]_3[Re_7C(CO)_{21}]$ in the presence of CO but without PPh_3 provides $[PPN][Re_7C(CO)_{22}]$ in high yield (89%). Decapping of [PP-

Table II. Selected Positional Parameters for $[PPN]_2[Re_6C(CO)_{19}]\cdot 2C_3H_6O$

	x/a	*y/b*	*z/c*
Re1	0.30190 (3)	0.05921 (5)	0.56898 (3)
Re2	0.26956 (6)	−0.08299 (9)	0.49061 (5)
Re3	0.23352 (6)	0.19128 (9)	0.51732 (5)
Re4	0.32074 (6)	0.0889 (1)	0.46307 (5)
Re5	0.18219 (6)	0.0123 (1)	0.54474 (5)
C	0.2500	0.054 (2)	0.5000
O11	0.4127 (5)	0.1640 (9)	0.5772 (6)
O12	0.3680 (6)	−0.0878 (8)	0.6283 (5)
O13	0.2696 (6)	0.1754 (9)	0.6587 (5)
O14	0.240 (1)	−0.050 (2)	0.656 (1)
O21	0.203 (2)	−0.232 (2)	0.433 (1)
O22	0.3692 (9)	−0.150 (2)	0.433 (1)
O23	0.293 (2)	−0.218 (2)	0.5780 (9)
O31	0.186 (1)	0.315 (2)	0.4319 (9)
O32	0.321 (1)	0.336 (2)	0.545 (1)
O33	0.157 (1)	0.278 (2)	0.5918 (10)
O41	0.334 (1)	0.031 (2)	0.3523 (5)
O42	0.4444 (5)	0.039 (2)	0.481 (1)
O43	0.353 (1)	0.2828 (10)	0.440 (1)
O51	0.0628 (6)	0.008 (2)	0.495 (1)
O52	0.152 (1)	−0.180 (1)	0.574 (1)
O53	0.129 (1)	0.095 (2)	0.6368 (8)
C11	0.3690 (6)	0.126 (1)	0.5737 (8)
C12	0.3407 (8)	−0.031 (1)	0.6068 (7)
C13	0.2836 (8)	0.130 (1)	0.6250 (6)
C14	0.241 (2)	−0.013 (3)	0.611 (2)
C21	0.226 (2)	−0.170 (3)	0.454 (2)
C22	0.332 (1)	−0.115 (3)	0.454 (2)
C23	0.284 (2)	−0.172 (3)	0.540 (2)
C31	0.210 (2)	0.278 (2)	0.469 (1)
C32	0.289 (2)	0.270 (3)	0.544 (2)
C33	0.180 (1)	0.237 (3)	0.560 (1)
C41	0.327 (2)	0.058 (3)	0.3939 (6)
C42	0.3954 (7)	0.054 (3)	0.478 (1)
C43	0.342 (2)	0.207 (1)	0.448 (2)
C51	0.1101 (8)	0.008 (3)	0.512 (1)
C52	0.166 (2)	−0.108 (1)	0.560 (2)
C53	0.144 (2)	0.067 (2)	0.597 (1)

Table III. Selected Bond Distances (Å) and Angles (deg) for the Cluster Anion in $[PPN]_2[Re_6C(CO)_{19}]\cdot 2C_3H_6O$

Distances			
Re1–Re2	3.015 (2)	Re1′–Re2	3.083 (2)
Re1–Re3	2.845 (2)	Re1′–Re3	3.073 (2)
Re1–Re4	2.871 (2)	Re1′–Re4	3.033 (2)
Re1–Re5	2.978 (2)	Re1′–Re5	3.104 (2)
Re2–Re4	2.950 (2)	Re3–Re4	3.015 (2)
Re2–Re5	2.965 (2)	Re3–Re5	3.042 (2)
$Re–C_{carbide}$	2.121 (4)(avg)	Re1′–C14′	2.18 (4)
Re1–C14	2.18 (4)	Re2–C14′	2.86 (4)
Re5–C14	2.20 (4)	Re4–C14′	2.81 (4)

Angles			
Re2–Re1–Re3	92.82 (4)	Re2–Re1–Re4	60.11 (4)
Re2–Re1–Re5	59.30 (4)	Re3–Re1–Re4	63.67 (4)
Re3–Re1–Re5	62.95 (4)	Re3–Re1–Re5	92.32 (4)
Re1–Re2–Re4	57.52 (4)	Re1–Re2–Re5	59.73 (4)
Re1–Re2–Re1′	88.27 (4)	Re4–Re2–Re5	91.01 (5)
Re4–Re2–Re1′	60.32 (4)	Re5–Re2–Re1′	61.73 (4)
Re1–Re3–Re4	58.58 (4)	Re1–Re3–Re5	60.66 (4)
Re4–Re3–Re5	88.30 (5)	Re1–Re3–Re1′	91.62 (4)
Re5–Re3–Re1′	61.00 (4)	Re4–Re3–Re1′	59.75 (4)
Re1–Re4–Re3	57.75 (4)	Re1–Re4–Re2	62.37 (4)
Re2–Re4–Re3	90.75 (5)	Re1–Re4–Re1′	91.94 (4)
Re3–Re4–Re1′	61.07 (4)	Re2–Re4–Re1′	62.00 (4)
Re1–Re5–Re3	56.39 (4)	Re1–Re5–Re2	60.97 (4)
Re2–Re5–Re3	89.95 (5)	Re1–Re5–Re1′	88.54 (4)
Re3–Re5–Re1′	59.99 (4)	Re2–Re5–Re1′	61.01 (4)
Re2–Re1′–Re4	57.68 (4)	Re2–Re1′–Re3	87.22 (4)
Re–Re1′–Re4	59.18 (4)	Re2–Re1′–Re5	57.26 (4)
Re3–Re1′–Re5	59.01 (4)	Re4–Re1′–Re5	86.86 (4)
Re1–Re5–C14	47 (1)	Re1–C14–O14	136 (3)
Re1–C14–Re5	86 (1)	Re5–C14–O14	138 (3)
Re1′–C14′–Re2	74 (1)	Re1′–C14′–O14′	136 (3)
Re1′–C14′–Re4	74 (1)	Re2–C14′–O14′	133 (3)
Re2–C14′–Re4	62.7 (8)	Re4–C14′–O14′	145 (3)

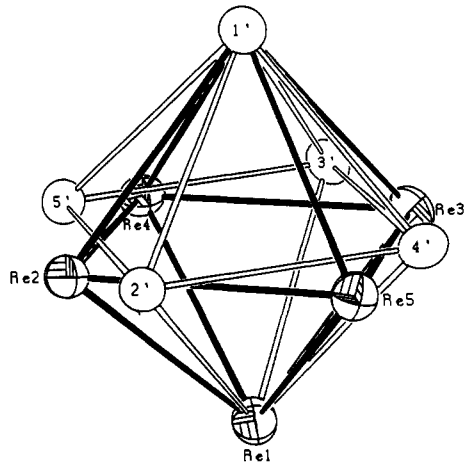

Figure 1. Diagram of the disordered Re_6 core in $[PPN]_2[Re_6C(CO)_{19}]$ showing the crystallographically imposed C_2 symmetry.

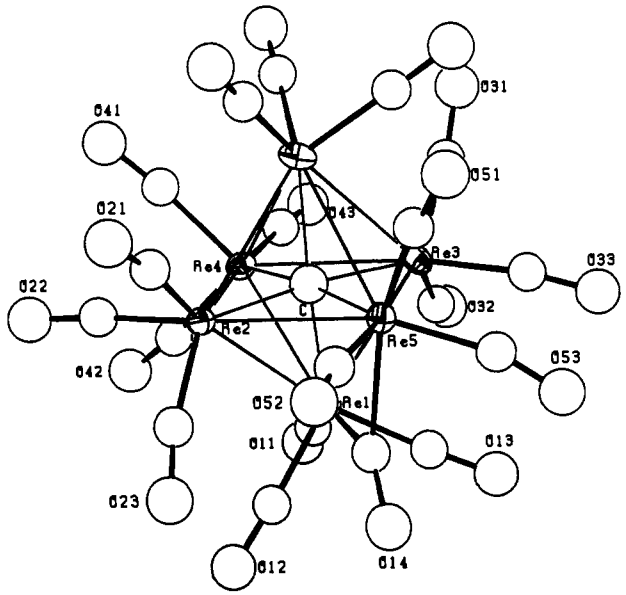

Figure 2. ORTEP diagram (35% probability ellipsoids) of $[Re_6C(CO)_{19}]^{2-}$ showing the edge-bridging orientation for carbonyl C14–O14. The Re–C distances involving this carbonyl are Re1–C14 = 2.18 (4) Å and Re5–C14 = 2.20 (4) Å.

N][$Re_7C(CO)_{22}$] with excess triphenylphosphine in acetone also gives $[PPN]_2[Re_6C(CO)_{19}]$ in ca. 90% yield, but this reaction requires ca. 48 h to complete, compared with 5–6 h for the oxidative-decapping reaction starting with $[PPN]_3[Re_7C(CO)_{21}]$.

From X-ray data obtained at −125 °C, the crystal structure of $[PPN]_2[Re_6C(CO)_{19}]$ was solved in the monoclinic space group *I2/a*. Details are provided in Table I. The cluster anion has crystallographically imposed C_2 symmetry, and the resulting symmetry-related positions for the octahedral Re_6 core are shown in Figure 1. Each metal atom is bonded to three terminal carbonyl ligands; however, there are two unique positions for carbonyl C14–O14, in which it is associated with either an edge or a face of the Re_6 octahedron. Figure 2 is an ORTEP diagram of the anion showing the edge-bridging orientation for carbonyl C14–O14. Figure 3 is an analogous diagram for the alternative face-bridging carbonyl location. Selected bond distances and angles for the cluster complex are given in Table III.

Figure 4 shows the ^{13}C NMR (125 MHz) spectrum of $[PPN]_2[Re_6{}^{13}C(^{13}CO)_{19}]$, with resonances for the carbide ligand and for the exchange-averaged carbonyl ligands at δ 417.9 (1 C) and 198.0 (19 C), respectively. Insert a shows an expansion of the carbonyl region, and insert b shows the same region recorded while irradiating the carbide signal. The apparent "triplet" in insert a is a superposition of a singlet and a doublet due to ^{13}C–^{13}C coupling of the carbide to the exchange-averaged carbonyls ($^2J_{av}$

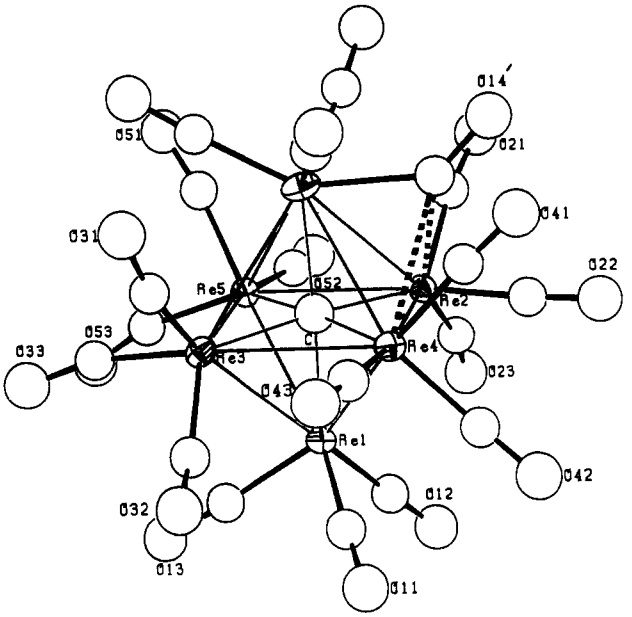

Figure 3. ORTEP diagram (35% probability ellipsoids) of $[Re_6C(CO)_{19}]^{2-}$ showing the face-bridging configurations for carbonyl C14′–O14′. The Re–C distances involving this ligand are Re1′–C14′ = 2.18 (4) Å, Re2–C14′ = 2.86 (4) Å, and Re4–C14′ = 2.81 (4) Å.

= 2.6 Hz). The offset between the centers of the two signals is 0.25 Hz; thus, the $^{13}C/^{12}C$ isotope effect of the carbide is 2 ppb. Inserts c and d show the carbonyl resonance recorded at 75 MHz and, respectively, at 25 and −85 °C.

Discussion

Formation of $[Re_6C(CO)_{19}]^{2-}$. It was previously reported that the oxidation of $[Re_7C(CO)_{21}]^{3-}$ with 2 equiv of $[C_7H_7]^+$ in the presence of carbon monoxide formed $[Re_7C(CO)_{22}]^-$,[7] and we have duplicated this result with $[Cp_2Fe]^+$ as the oxidant. However, we have found that the analogous oxidation of $[Re_7C(CO)_{21}]^{3-}$ in the presence of excess triphenylphosphine provides a route to $[Re_6C(CO)_{19}]^{2-}$ in high yield. $[Re_7C(CO)_{22}]^-$ is not an intermediate in the formation of $[Re_6C(CO)_{19}]^{2-}$ under these conditions, since the direct conversion of $[Re_7C(CO)_{22}]^-$ to $[Re_6C(CO)_{19}]^{2-}$ with triphenylphosphine occurs at a much slower rate. It appears likely that carbon monoxide and triphenylphosphine compete for the same reactive intermediate and that a large excess of the phosphine is needed to block the formation of $[Re_7C(CO)_{22}]^-$ as well as to induce the subsequent fragmentation.

On the other hand, the presence of carbon monoxide in the reaction mixture is necessary for the highest yields of $[Re_6C(CO)_{19}]^{2-}$, since lower yields are realized under a nitrogen atmosphere. This requirement for exogeneous CO may signify that the departing mononuclear rhenium cation has at least three carbonyl ligands. However, even though triphenylphosphine is present in a 20–40-fold excess, the mononuclear coproduct that is observed is the disubstituted complex $[Re(CO)_4(PPh_3)_2]^+$. This result is consistent with previous studies on phosphine substitution reactions of $[Re(CO)_6]ClO_4$,[8] in that reaction with triphenylphosphine failed to give a trisubstituted complex, presumably for steric reasons.

In the reported conversion of $[Re_7C(CO)_{21}]^{3-}$ to $[Re_6C(CO)_{19}]^{2-}$ by the action of iodine in the presence of carbon monoxide,[1] iodide is incorporated into a further degradation product, $[Re_4C(CO)_{15}I]^-$. Studies on various osmium clusters have shown clearly that iodine can act either as an "outer-sphere" two-electron oxidant or as an "inner-sphere" reagent where the coordination of an iodide ligand results in the breaking of metal–metal bonds and opening up of the metal polyhedron.[9] Our decapping reaction of $[Re_7C(CO)_{21}]^{3-}$, utilizing the ferrocenium ion and triphenylphosphine, effectively separates the oxidative and nucleophilic roles of the iodine/iodide reagent, resulting in an alternative means of cluster fragmentation, which in this case is quite selective and efficient.

Solid-State Structure of $[PPN]_2[Re_6C(CO)_{19}]$. In accord with the preliminary report by Beringhelli et al.,[1] the structure we have determined for $[PPN]_2[Re_6C(CO)_{19}]$ shows an octahedral rhenium unit with the carbide ligand inside the cavity. The average rhenium–carbide distance (2.12 Å) as well as the metal–metal distances are in accord with those of other $Re_n(\mu_6\text{-}C)$ clusters.[2,5,7,10,11] Despite the 2-fold disorder of the Re_6 framework in the solid state (see Figure 1), 18 of the carbonyl ligands are clearly terminal, three per metal atom. However, two distinct sites for the 19th carbonyl (C14–O14) relative to the Re_6 core are observed.

Figure 2 shows one configuration, which places the unique carbonyl in a symmetrically edge-bridging position between Re1 and Re5. The Re–C distances involving this carbonyl (Re1–C14 = 2.18 (4) Å and Re5–C14 = 2.20 (4) Å) are indistinguishable from those involving the edge-bridging carbonyl in the structure of $[NEt_4][Re_7C(CO)_{22}]$ (average Re–C(O) = 2.19 (1) Å).[7] Indeed, this configuration for $[Re_6C(CO)_{19}]^{2-}$ can be viewed as being directly related to the structure of $[Re_7C(CO)_{22}]^-$ by simply removing the "$Re(CO)_3^+$ cap" from the latter (see structure I and II).

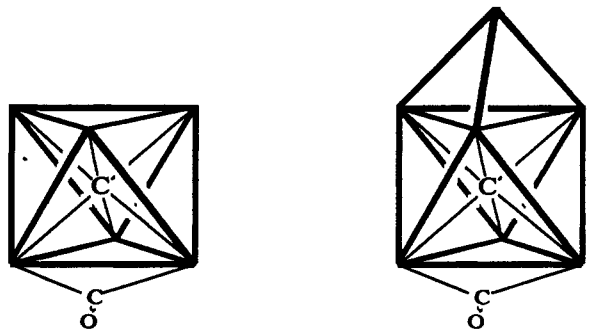

I II

In the alternative face-bridging position shown in Figure 3, the carbonyl C14′–O14′ is associated with the triangular face formed by Re1′, Re2, and Re4. The shortest rhenium–carbon (Re1′–C14′) distance is 2.18 Å, and the other two rhenium–carbon (Re2–C14′ and Re4–C14′) distances are 2.86 and 2.81 Å, respectively. In effect, the carbonyl is semibridging with respect to Re2 and Re4. The only reported example of a semibridging carbonyl ligand in a rhenium cluster is in $[NEt_4]_2[HRe_5C(CO)_{16}]$.[4] In this compound, the unique carbonyl is located on a basal–apical edge of the square pyramidal cluster framework, with the basal rhenium–carbon distance = 2.20 (5) Å, the apical rhenium–carbon distance = 2.52 (10) Å, and the basal rhenium–carbon–oxygen angle = 150 (9)°. To the best of our knowledge there has been no previous example of a face-bridging carbonyl ligand in a rhenium cluster.

The combination of 19 carbonyl ligands and an octahedral arrangement of metal atoms is unique to $[Re_6C(CO)_{19}]^{2-}$. Previous structural studies have shown that the cluster compounds with 19 carbonyl ligands have either relatively open polyhedral structures, as in $Os_5(CO)_{19}$ (bowtie)[12] and $H_2Os_6(CO)_{19}$ (edge-bridged TBP),[13] or a larger metal framework, such as $Rh_8C(CO)_{19}$

(7) Beringhelli, T.; D'Alfonso, G.; De Angelis, M.; Ciani, G.; Sironi, A. *J. Organomet. Chem.* **1987**, *322*, C21.
(8) Abel, E. W.; Tyfield, S. P. *Can. J. Chem.* **1969**, *47*, 4627.
(9) Goudsmit, R. J.; Johnson, B. F. G.; Lewis, J.; Nelson, W. J. H.; Vargas, M. D.; Braga, D.; McPartlin, M.; Sironi, A. *J. Chem. Soc., Dalton Trans.* **1985**, 1795 and references therein.
(10) Ciani, G.; D'Alfonso, G.; Freni, M.; Romiti, P.; Sironi, A. *J. Chem. Soc., Chem. Commun.* **1982**, 705.
(11) Beringhelli, T.; D'Alfonso, G.; Ciani, G.; Sironi, A.; Molinari, H. *J. Chem. Soc., Dalton Trans.* **1988**, 1281.
(12) Farrar, D. H.; Johnson, B. F. G.; Lewis, J.; Raithby, P. R.; Rosales, M. J. *J. Chem. Soc., Dalton Trans.* **1982**, 2051.

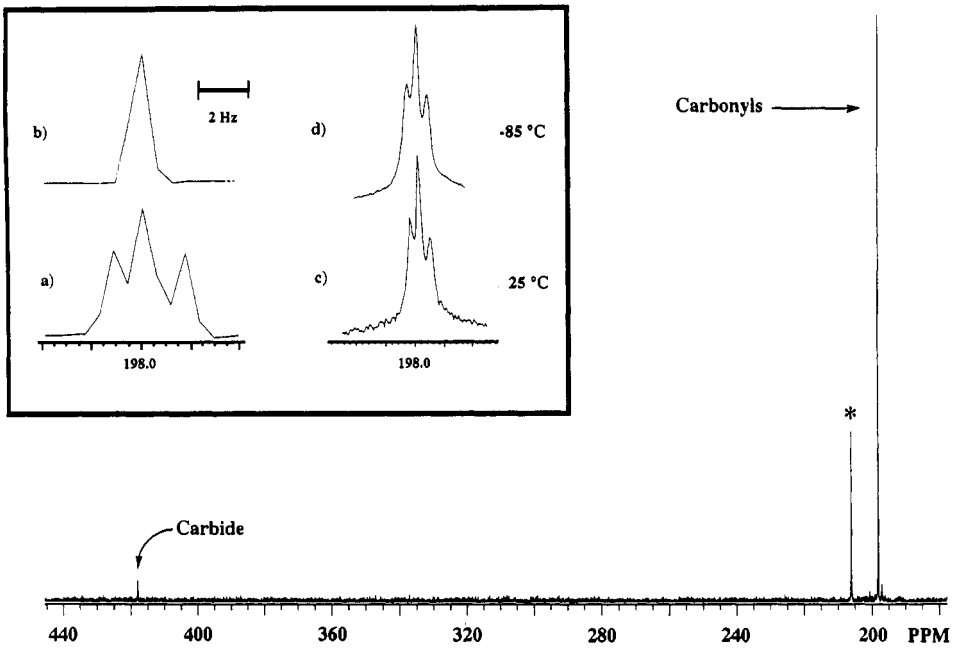

Figure 4. ^{13}C NMR spectrum of ^{13}C-enriched $[Re_6C(CO)_{19}]^{2-}$. The carbide and averaged carbonyl resonance are at δ 417.9 (1 C) and 198.0 (19 C), respectively. Insert a shows the expanded carbonyl region at 125 MHz. Insert b shows the same region as in insert a with simultaneous irradiation at the carbide signal. Inserts c and d show the 75-MHz spectra at +25 and −85 °C, respectively. The asterisk marks an acetone solvent resonance.

Table IV. Selected Oxygen–Oxygen Distances (Å) for the Cluster Anion in $[PPN]_2[Re_6C(CO)_{19}]\cdot 2C_3H_6O$

O11–O12	4.15 (3)	O11′–O12′	4.15 (3)
O11–O13	4.16 (3)	O11′–O13′	4.16 (3)
O12–O13	4.68 (3)	O12′–O13′	4.68 (3)
O21–O22	4.23 (4)	O31–O32	4.32 (4)
O21–O23	4.28 (5)	O31–O33	4.31 (5)
O22–O23	4.54 (4)	O32–O33	4.24 (4)
O41–O42	4.11 (4)	O51–O52	4.00 (3)
O41–O43	4.42 (4)	O51–O53	4.07 (4)
O42–O43	4.23 (5)	O52–O53	4.42 (4)
O14–O12	3.25 (4)	O14–O52	3.45 (4)
O14–O13	3.44 (4)	O14–O53	3.37 (5)
O14–O23	3.37 (5)		

(square antiprism)[14] and $Rh_9(CO)_{19}$ (stacked triangles).[15] Octahedral cluster compounds of rhenium, ruthenium, and osmium with up to 18 carbonyl ligands have been characterized crystallographically, including $[H_2Re_6C(CO)_{18}]^{2-}$,[5] $[Ru_6(CO)_{18}]^{2-}$,[16] $[HRu_6(CO)_{18}]^-$,[17] $H_2Ru_6(CO)_{18}$,[18] $[Os_6(CO)_{18}]^{2-}$,[19] and $[HOs_6(CO)_{18}]^-$.[19] With the exception of $[Ru_6(CO)_{18}]^{2-}$, which has two μ_2- and two μ_3-carbonyl ligands, the octahedral cluster compounds have three terminal carbonyl ligands bonded to each metal atom. This is in accord with Mingo's cluster cone angle concept as applied to an octahedral metal framework with M–M distances of ca. 2.90 Å.[20] However, the Re–Re distances in $[Re_6C(CO)_{19}]^{2-}$ have an average value of 3.00 Å, which apparently allows a higher limit on the number of carbonyl ligands.

An alternative view of the structures of binary metal carbonyl clusters focuses on the nonbonded repulsions within the carbonyl ligand shell as a whole, and Johnson and Benfield have carried out "points-on-a-sphere" calculations for possible configurations of up to 16 carbonyls.[21,22] A quantitative treatment for 19 carbonyl ligands would likely stretch the assumptions of this method. Nevertheless, the structure of $[Re_6C(CO)_{19}]^{2-}$ can be analyzed qualitatively by considering the displacement of the 18 terminal carbonyl ligands caused by addition of the 19th carbonyl, and one view of the intercarbonyl repulsions is given by the pattern of the nonbonded oxygen–oxygen distances. Figure 5 shows the polyhedron of oxygen atoms for the edge-bridged configuration, with the solid lines indicating the sets of three terminal carbonyl ligands bonded to each metal atom and the dashed lines denoting O14 and its nearest neighbors. The indicated oxygen–oxygen distances are listed in Table IV. The triangles of oxygen atoms that are closest to O14 are not equilateral. For instance, the triangle (O11, O12, O13) has O12–O13 = 4.68 Å as the longest side compared to the other two sides, O11–O12 = 4.15 Å and O11–O13 = 4.16 Å. As seen by the two very short distances from

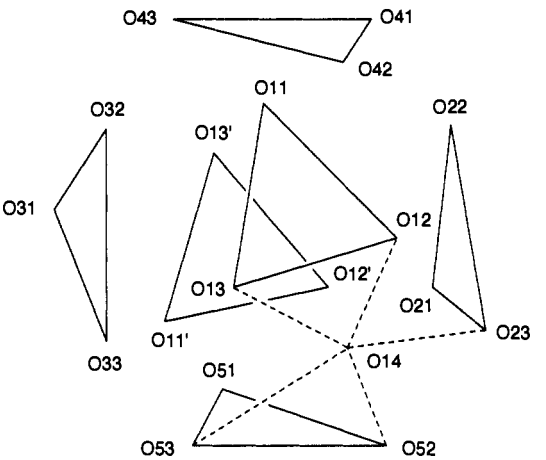

Figure 5. Polyhedron of oxygen atoms from the carbonyl ligands. Lines are drawn to indicate the oxygen–oxygen distances between the carbonyl ligands bonded to the same metal atom, based on the edge-bridging configuration shown in Figure 2, and between O14 and its nearest neighbors.

(13) Johnson, B. F. G.; Khattar, R.; Lewis, J.; McPartlin, M.; Morris, J.; Powell, G. L. *J. Chem. Soc., Chem. Commun.* **1986**, 507.
(14) Albano, V. G.; Sansoni, M.; Chini, P.; Martinengo, S.; Strumolo, D. *J. Chem. Soc., Dalton Trans.* **1975**, 305.
(15) Martinengo, S.; Fumagalli, A.; Bonfichi, R.; Ciani, G.; Sironi, A. *J. Chem. Soc., Chem. Commun.* **1982**, 825.
(16) Jackson, P. F.; Johnson, B. F. G.; Lewis, J.; McPartlin, M; Nelson, W. J. H. *J. Chem. Soc., Chem. Commun.* **1979**, 735.
(17) Eady, C. R.; Jackson, P. F.; Johnson, B. F. G.; Lewis, J.; Malatesta, M. C.; McPartlin, M.; Nelson, W. J. H. *J. Chem. Soc., Dalton Trans.* **1980**, 383.
(18) Churchill, M. R.; Wormald, J. *J. Am. Chem. Soc.* **1971**, *93*, 5670.
(19) McPartlin, M.; Eady, C. R.; Johnson, B. F. G.; Lewis, J. *J. Chem. Soc. Chem. Commun.* **1976**, 883.
(20) Mingos, D. M. P. *Inorg. Chem.* **1982**, *21*, 464.
(21) Benfield, R. E.; Johnson, B. F. G. *J. Chem. Soc., Dalton Trans.* **1980**, 1743.
(22) Johnson, B. F. G.; Benfield, R. E. *Top. Stereochem.* **1981**, *12*, 253.

O14 to O12 and O13 (3.25 and 3.44 Å, respectively), the two carbonyls C12–O12 and C13–O13 are significantly displaced from idealized positions by carbonyl C14–O14. In triangle (O51, O52, O53) and triangle (O21, O22, O23), there are also longer oxygen–oxygen distances associated with the oxygen(s) that are close to O14. Collectively there are five relatively short oxygen–oxygen distances involving O14, and these are taken to indicate the significant interligand repulsions associated with carbonyl C14–O14. In contrast, the triangle (O31, O32, O33), formed by oxygens of carbonyls that are not in close proximity to carbonyl C14–O14, is almost an equilateral triangle.

Solution Stereodynamics of $[PPN]_2[Re_6C(CO)_{19}]$. The infrared spectra (ν_{CO}) determined for $[PPN]_2[Re_6C(CO)_{19}]$ are very similar in solution and in the solid state. In particular, a band at 1815 cm^{-1} (CH_2Cl_2) or 1810 cm^{-1} (KBr) can be attributed to a bridging carbonyl in each case. This compares well with an analogous band observed for $[PPN][Re_7C(CO)_{22}]$ at 1843 cm^{-1} (CH_2Cl_2), when the effect of the unit change in charge is taken into account. However, it is not clear whether both structural forms observed for $[PPN]_2[Re_6C(CO)_{19}]$ in the solid state are present also in solution, since no structure-limiting information was obtained from the ^{13}C NMR spectrum even at −85 °C (see Figure 4d). The high degree of fluxionality displayed by $[PPN]_2[Re_6C(CO)_{19}]$ in solution could result from the facile interconversion of two alternative orientations of the octahedral metal core within the carbonyl ligand ensemble, as seen in the solid-state structure.[23,24] However, $[Re_7C(CO)_{22}]^-$ also shows rapid and complete scrambling of the carbonyl ligands at room temperature,[25] and no disorder was mentioned in the reported crystallographic study.[7] Furthermore, other derivatives of the "$Re_6C(CO)_{18}$" core, e.g., $[Re_7C(CO)_{21}]^{3-}$,[2] $[Re_8C(CO)_{24}]^{2-}$,[10] and $[Re_7C(CO)_{21}ML_n]^{2-}$,[26] none of which has more than three carbonyls per metal atom, show no evidence for rapid carbonyl migration on the metal framework. Thus, the steric repulsions resulting from an "excess" number of carbonyl ligands, with the attendant reduction in strongly directional bonding, are probably responsible for the fluxionality displayed by both $[Re_6C(CO)_{19}]^{2-}$ and $[Re_7C(CO)_{22}]^-$.

Photoinduced Substitution Reaction of $[PPN]_2[Re_6C(CO)_{19}]$ with Dihydrogen. In spite of the obvious steric interactions in the structure of $[PPN]_2[Re_6C(CO)_{19}]$, the compound does not dissociate a carbonyl ligand under mild thermal conditions. In particular, it does not react with H_2 to give the known derivative $[PPN]_2[H_2Re_6C(CO)_{18}]$[3,5] before it begins to decompose at ca. 150 °C. However, photoinduced hydrogenation of $[PPN]_2[Re_6C(CO)_{19}]$ to $[PPN]_2[H_2Re_6C(CO)_{18}]$ does occur cleanly at room temperature with just sunlamp irradiation. This is especially remarkable in that most large metal carbonyl clusters have appeared to be inert to photoinduced carbonyl ligand substitution,[27-29] even though they are often intensely colored. We assume that this unusual reaction proceeds through an unsaturated cluster intermediate of the formula $[Re_6C(CO)_{18}]^{2-}$ and that the expected high symmetry and low steric repulsions of such a species may be important elements in its facile formation. Efforts to characterize such an intermediate by additional reactions are ongoing.

Acknowledgment. This research was supported by grants from the National Science Foundation (CHE 89-15349 to J.R.S. and DMR 89-20538 to the Materials Research Laboratory). We thank Makoto Koike for assistance with the decoupling experiment and Dr. Scott D. Kahn for providing a copy of his MacModel graphics program.

Supplementary Material Available: A description of the crystallographic details and tables of equivalent positions, atomic positional parameters, thermal parameters, and bond distances and angles (22 pages); a stable of final observed and calculated structure factors (20 pages). Ordering information is given on any current masthead page.

(23) Johnson, B. F. G.; Benfield, R. E. In *Transition Metal Clusters*; Johnson, B. F. G., Ed.; Wiley: New York, 1980; Chapter 7, p 471.
(24) Johnson, B. F. G.; Rodgers, A. In *The Chemistry of Metal Cluster Complexes*; Shriver, D. F., Kaesz, H. D., Adams, R. D., Eds.; VCH: New York, 1990; Chapter 6, p 303.
(25) Simerly, S. W.; Shapley, J. R. *Inorg. Chem.* **1990**, *29*, 3634.
(26) Henly, T. J.; Shapley, J. R.; Rheingold, A. L.; Geib, S. J. *Organometallics* **1988**, *7*, 441.
(27) For example, $[Re_8C(CO)_{24}]^{2-}$ is inert to photoinduced substitution in THF even though the mononuclear analogue $CpRe(CO)_3$ readily forms $CpRe(CO)_2(THF)$: Folkers, J. P.; Shapley, J. R. Unpublished observations.
(28) Photosubstitution has been studied extensively for $Os_3(CO)_{12}$: Bentsen, J. G.; Wrighton, M. S. *J. Am. Chem. Soc.* **1987**, *109*, 4518 and references therein.
(29) For the photoextrusion of mercury from $[Os_{18}Hg_3C_2(CO)_{42}]^{2-}$, see: Charalambous, E.; Gade, L. H.; Johnson, B. F. G.; Kotch, T.; Lees, A. J.; Lewis, J.; McPartlin, M. *Angew. Chem., Int. Ed. Engl.* **1990**, *29*, 1137.

Contribution from the Department of Chemistry, University of Calgary, Calgary, Alberta, Canada T2N 1N4

C–S Bond Cleavage in Tris(μ-thioether)ditungsten(III) Complexes in Reactions with Anionic Nucleophiles, Including Hydride: Synthesis and Structure of $[PPh_4][Cl_3W(\mu\text{-}THT)_2(\mu\text{-}S(CH_2)_4Cl)WCl_3]$ and $Na[Cl_3W(\mu\text{-}SEt_2)_2(\mu\text{-}SEt)WCl_3]\cdot 3THF$

P. Michael Boorman,* Xiaoliang Gao, James F. Fait, and Masood Parvez

Received September 18, 1990

The bridging thioether ligands in the complexes $Cl_3W(\mu\text{-}Et_2S)_3WCl_3$ (**1**) and $Cl_3W(\mu\text{-}THT)_3WCl_3$ (**2**) (THT = tetrahydrothiophene) are highly susceptible to nucleophilic attack by the anions X^- (X = SR^-, SeR^-, Cl^-, Br^-, H^-), resulting in the cleavage of a C–S bond. Attack on **1** yields complexes containing the deethylated anion $[Cl_3W(\mu\text{-}SEt)(\mu\text{-}SEt_2)_2WCl_3]^-$, and the byproducts EtX. Nucleophilic attack on the THT in **2** results in ring opening to give functionalized μ-thiolate anions of general formula $[Cl_3W(\mu\text{-}THT)_2(\mu\text{-}S(CH_2)_4X)WCl_3]^-$. The yields of these derivatives are essentially quantitative. Crystal structures of two representative derivatives are reported. $Na[Cl_3W(\mu\text{-}SEt)(\mu\text{-}SEt_2)_2WCl_3]\cdot 3THF$ (**3a**) crystallizes in the triclinic space group $P\bar{1}$ with a = 11.306 (1) Å, b = 12.750 (1) Å, c = 14.936 (1) Å, α = 91.990 (9)°, β = 105.180 (8)°, γ = 114.530 (8)°, V = 1865.0 (4) Å^3, Z = 2, d_c = 1.890 g/cm^3, μ(Mo Kα) = 69.24 cm^{-1}, R = 0.061, and R_w = 0.079 for 274 parameters and 6229 unique data having $F > 4.0\sigma(F)$. $[PPh_4][Cl_3W(\mu\text{-}THT)_2(\mu\text{-}S(CH_2)_4Cl)WCl_3]$ (**4**) crystallizes in the monoclinic space group $P2_1/n$ with a = 8.952 (3), b = 18.136 (5), c = 26.525 (5) Å, β = 94.43 (2)°, V = 4293.56 Å^3, Z = 4, d_c = 1.887 g/cm^3, μ(Mo Kα) = 58.5 cm^{-1}, R = 0.040, and R_w = 0.045 for 433 parameters and 5956 unique data having $I > 3\sigma(I)$. The anions in both **3a** and **4** have a confacial bioctahedral framework in which one of the μ-thioether ligands in the precursor complexes has been converted to a μ-thiolate. The reaction between hydride and **1** or **2** is a possible model for hydrodesulfurization.

Introduction

The activation of C–S bonds in coordinated organosulfur ligands is of interest in connection with the modeling of catalytic hydrodesulfurization (HDS) reactions. We report here on a rare example of a stoichiometric, facile C–S bond cleavage in a μ-thioether ligand that may provide a mechanism by which thioethers

